

Modeling a Dew Point Indirect Evaporative Cooling System for TRNSYS Building Simulations: Proposal and Validation

Alessandra Urso – University of Catania, Italy / University of Valladolid, Spain – alessandra.urso@phd.unict.it

Gianpiero Evola – University of Catania, Italy – gianpiero.evola@unict.it

Francesco Nocera – University of Catania, Italy – francesco.nocera@unict.it

Vincenzo Costanzo – University of Catania, Italy – vincenzo.costanzo@unict.it

Ana Tejero-Gonzales – University of Valladolid, Spain – ana.tejero@uva.es

Eloy Velasco-Gomez – University of Valladolid, Spain – eloy.velasco.gomez@uva.es

Abstract

This paper aims to develop a mathematical model of a dew-point indirect evaporative cooler that can be easily implemented in a TRNSYS building simulation environment. The model is validated against experimental data from a tested mixed flow prototype. The results show that the model is consistent with the experiments with an error in the primary air temperature drop between 12% and 18%. Furthermore, a parametric analysis is performed to evaluate the effect of the size of the device. The temperature drop may double by increasing three times the height or the width of the device. In conclusion, this study reveals the importance of a proper calculation of the Nusselt Number, especially for the wet channel.

1. Introduction

In order to reduce the cooling energy consumption in buildings and the greenhouse emissions during the whole lifecycle of the cooling systems, efforts should be made to improve their effectiveness and reduce their environmental impact. In this direction, conventional cooling systems that are based on vapor compression cycles and use chemical refrigerants may not be the best solution in terms of energy-saving and carbon neutrality. Among the possible alternative cooling systems, evaporative coolers have gained interest in recent years due to the possibility of cooling down the ambient air by taking advantage of water evaporation: today, they mainly find application as a stand-alone system, but also in combination with other cooling devices.

A particular kind of evaporative cooler is called a “dew point indirect evaporative cooler” (DPIEC). Being an indirect evaporative cooler, it consists in a heat exchanger composed of two distinct and adjacent channels: the primary air stream flows in the dry channel, while the secondary air stream flows in the wet channel where it comes in contact with water. Differently from direct evaporative cooling systems – where water is sprayed directly in the primary air– this technology does not increase the humidity ratio of the supply air. Furthermore, a DPIEC has the advantage of providing high performance in terms of temperature drop between primary air inlet and outlet. In fact, in direct and conventional indirect evaporative coolers the temperature drop can approach the wet bulb depression; instead, in a DPIEC the primary air outlet temperature can ideally achieve the dew point temperature associated with the inlet conditions. This happens because in the DPIEC a portion of the primary air in the dry channel is diverted into the wet channel to form the secondary air flow, which allows secondary air to be pre-cooled.

Although dew point evaporative coolers were largely investigated at component level, few studies focused on the performance ensured by a building where the system is applied. This gap could probably be due to the absence of a component able to properly simulate a dew-point indirect evaporative cooler in the common building simulation tools, such as TRNSYS. Indeed, a similar component –Type 757 of the TESS libraries – can model a conventional indirect evaporative cooler by

Part of

Pernigotto, G., Ballarini, I., Patuzzi, F., Prada, A., Corrado, V., & Gasparella, A. (Eds.). 2025. Building simulation applications BSA 2024. bu.press. <https://doi.org/10.13124/9788860462022>



knowing its wet bulb effectiveness. However, this component is not suitable to model a dew point indirect evaporative cooler, especially when its effectiveness is not known *a priori*. Therefore, this work aims to develop a mathematical model of a dew-point indirect evaporative cooler that can be easily implemented in TRNSYS building simulation environment. The mathematical model is here described and validated against experimental data and allows predicting the outlet conditions of the supply air that can then be used as an input in the dynamic building simulations. Furthermore, based on the model, a parametric analysis is performed to evaluate the effect of the dimensions of the device.

2. Methodology

The mathematical model presented in this study relies on the mass and energy balance equations and on the logarithmic mean temperature difference method (Jie & Chua, 2023). By knowing the heat transfer area (A) and the heat transfer coefficient (K) of the heat exchanger, the model can apply to other DPEICs with different configurations. The code is written in Python programming language, so that it can be easily called in TRNSYS Simulations Studio by Type 169 (TRNSYS 18). The model is validated against experimental data from a mixed-flow prototype.

2.1 Description of the Dew Point Indirect Evaporative Cooling System

The following figures show a schematic representation of the DPEIC modelled in this study (Fig. 1) and a detail of dry and wet channel (Fig. 2). The DPEIC consists of a heat exchanger with adjacent dry (primary) and wet (secondary) channels. Firstly, the inlet air enters the dry channels and is sensibly cooled down by the secondary air. After that, a portion (η) of the primary air is diverted into the wet channels to form the secondary air, while the remaining portion ($1 - \eta$) of the primary air is blown to the indoor environment. Moreover, a water distributor irrigates the wet channels. In this way, the secondary air is evaporatively cooled down. The exceeding water falls in a tank where it

is stored. At the end, a pump allows the water to re-circulate from the tank up to the distributor. Fig. 3 shows the primary air path (IN \rightarrow OUT-1) and the secondary air path (OUT-1 \rightarrow OUT-2) in the psychometric chart; the inlet secondary air point corresponds to the outlet primary air conditions (OUT-1).

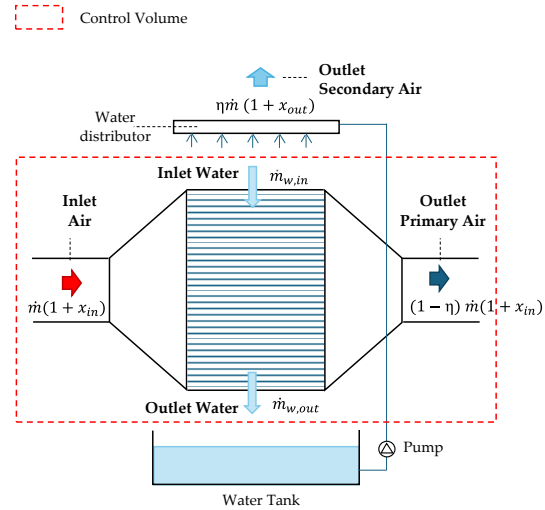


Fig. 1 – Schematic representation of DPEIC

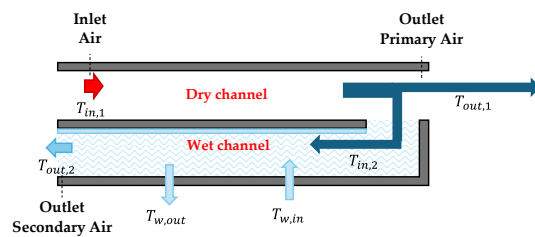


Fig. 2 – Schematic representation of dry and wet channels

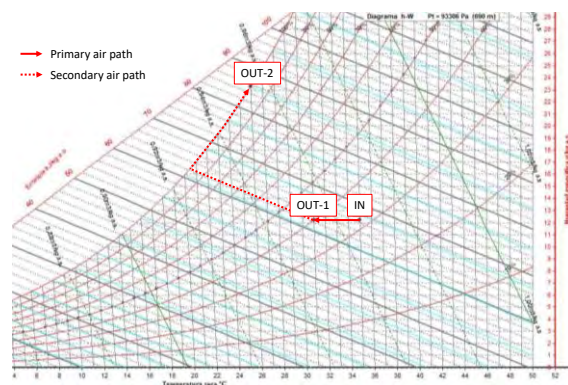


Fig. 3 – Psychometric chart from SICRO_V2_1_3 (University of Valencia, Spain)

2.2 Mathematical Development

The mathematical model developed here requires the following input data:

- the inlet air hygrometric conditions, in particular dry bulb temperature, relative humidity, and pressure;
- the inlet air mass flow rate;
- the features of the device, i.e. working-to-intake air ratio (η), heat transfer area, and heat transfer coefficient;
- the water inlet temperature.

Furthermore, the following assumptions hold:

- 1) steady-state conditions;
- 2) adiabatic heat exchanger;
- 3) saturation of the secondary air;
- 4) no water losses between primary and secondary channel (primary process perfectly at constant humidity ratio);
- 5) water temperature is known and constant.

The energy balance applies to the control volume indicated in Fig. 1 and is given by Eq. 1:

$$\begin{aligned} \dot{m}h_{in} + \dot{m}_{w,in}h_w &= \\ &= (1 - \eta)\dot{m}h_{out1} + \eta\dot{m}h_{out2} + \dot{m}_{w,out}h_w \end{aligned} \quad (1)$$

Here, \dot{m} is the inlet air mass flow rate, $\dot{m}_{w,in}$ is the inlet water mass flow, $\dot{m}_{w,out}$ is the outlet water mass flow, η is the working-to-intake air ratio, and h_{in} , h_{out1} , h_{out2} are the specific enthalpy values of the inlet humid air, the outlet primary humid air, and the outlet secondary humid air respectively. Finally, h_w is the specific enthalpy of the inlet and the outlet water that is considered constant, coherently with the steady-state hypothesis.

By introducing the mass balance in the secondary channel (Eq. 2), the energy balance can then be rewritten as in Eq. 3:

$$\begin{aligned} \dot{m}_{w,in} - \dot{m}_{w,out} &= \eta\dot{m}(x_{out} - x_{in}) = \eta\dot{m}\Delta x \quad (2) \\ h_{in} &= (1 - \eta)h_{out1} + \eta(h_{out2} - \Delta x \cdot h_w) \quad (3) \end{aligned}$$

With x_{in} inlet humidity ratio, x_{out} outlet humidity ratio and $\Delta x = x_{out} - x_{in}$. Therefore, the enthalpy of the primary outlet air is given by Eq. 4:

$$h_{out1} = \frac{h_{in} - \eta(h_{out2} - \Delta x \cdot h_w)}{(1 - \eta)} \quad (4)$$

This relation is not sufficient to solve the problem because the secondary outlet air conditions appear-

ing in Eq. 4 are not known. The equation can be solved iteratively by supposing an outlet secondary air temperature $T_{out,2}$ (which is sufficient to determine the associated enthalpy because of the hypothesis of saturation condition) and by finding a further equation to verify the exactness of this value. Such further equation can be derived by the logarithmic mean temperature difference method (Jie & Chua, 2023), in which the heat transfer rate between primary and secondary channel is given by Eq. 5:

$$\dot{q} = KA \cdot \Delta T_{lm} \quad (5)$$

Where K is the overall heat transfer coefficient and A is the heat transfer area. The logarithmic mean temperature difference ΔT_{lm} in a DPIEC is defined as in Eq. 6:

$$\Delta T_{lm} = \frac{\Delta T_1 - \Delta T_2}{\ln \frac{\Delta T_1}{\Delta T_2}} \quad (6)$$

With:

$$\Delta T_1 = T_{in1} - WBT_{out2} = T_{in} - T_{out2} \quad (7)$$

$$\Delta T_2 = T_{in2} - WBT_{in2} = T_{out1} - WBT_{out1} \quad (8)$$

In Eq. 7, the wet bulb temperature of the outlet secondary air (WBT_{out2}) is equal to its dry bulb temperature T_{out2} because of the assumption of saturated air in the secondary channel. Since the air conditions in the outlet of the primary channel are the same as the inlet of the secondary channel, in Eq. 8 the wet bulb temperature of the inlet secondary air WBT_{in2} is replaced with the outlet primary wet bulb temperature WBT_{out1} .

From the energy balance in the primary channel:

$$\dot{q} = \dot{m}(h_{out1} - h_{in}) = \dot{m}(c_a + x_{in}c_v)(T_{out1} - T_{in}) \quad (9)$$

Where c_a and c_v are the specific heat of dry air and water vapor, respectively, and x_{in} is the humidity ratio of the inlet air that is the same as the outlet primary air because of assumption 4. Therefore:

$$\dot{m}(c_a + x_{in}c_v)(T_{out1} - T_{in}) = KA \cdot \Delta T_{lm} \quad (10)$$

$$\Delta T_{lm} = \frac{\dot{m}(c_a + x_{in}c_v)}{KA} (T_{out1} - T_{in}) \quad (11)$$

In this way the result of Eq. 11 is compared with Eq. 6 until convergence. The method used to iteratively solve the problem is reported in more detail in the next subsection.

2.3 Mathematical Solution

The scheme in Fig. 4 shows the iterative method used to solve the above equations. A guess value for T_{out2} — lower than the inlet air temperature T_{in} —is assigned thus solving Eq. 4 and calculating h_{out1} , hence T_{out1} (inlet air has constant humidity ratio, corresponding to the inlet value). Then, two values of mean logarithmic difference temperature ΔT_{lm1} and ΔT_{lm2} are calculated by Eq. 6 and Eq. 11, respectively. The absolute value of their difference Δ is compared to a small threshold value (ϵ). If $\Delta \leq \epsilon$ the solution is found, otherwise the guess value of T_{out2} is incremented by δ and the scheme is repeated. In the following $\epsilon = 0.0001$ and $\delta = 0.005$ are adopted, respectively.

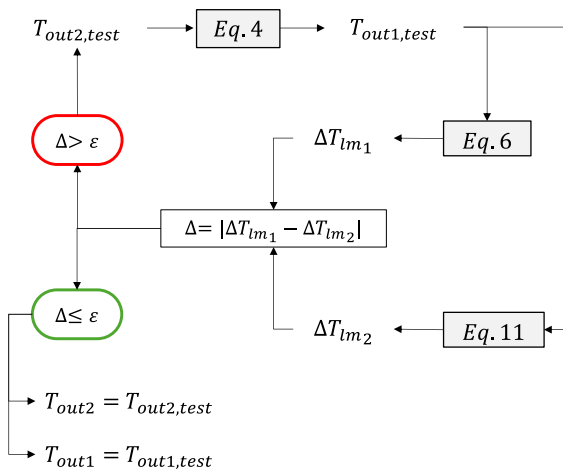


Fig. 4 – Step-by-step solution scheme

2.4 Description of the Experiment

In order to experimentally validate the mathematical model, a real small-scale prototype was built and tested. The device is composed of overlapped modular elements made with polycarbonate sheets. Each modular element consists of 28 dry channels and a wet plate. In the dry channels, some air paths are blocked, and holes are drilled along the plate to drive part of the primary air through the wet plate. The wet plate is covered with cotton cloth on one side. The upper side is open, thus allowing air to flow out and the water to be supplied. The bottom side, instead, is closed by a rib that is perforated to drain the excess water. Once assembled, the prototype is composed of eight modular elements. The design specifications are summed up in Table 1.

Table 1 – Design characteristics of the tested heat exchanger

Parameters	
Heat exchanger volume	31 x 25 x 30.5 cm
Heat transfer area	1.00 m ²
Flow configuration	Mixed flow
Dry channel length	30 cm
Dry channel width	9 mm
Dry channel height	9 mm
Number of dry channels	8
Wet channel length	30 cm
Wet channel height	30 cm
Wet channel gap	9 mm
Number of wet channels	8 x 28
Plate thickness	0.5 mm
Channel material	polycarbonate
Wicking material	cotton cloth

A water distributor is installed on the upper side and a water tank on the bottom side. A water pump allows the water to re-circulate from the tank to the distributor. Fig. 5 shows the test bench.

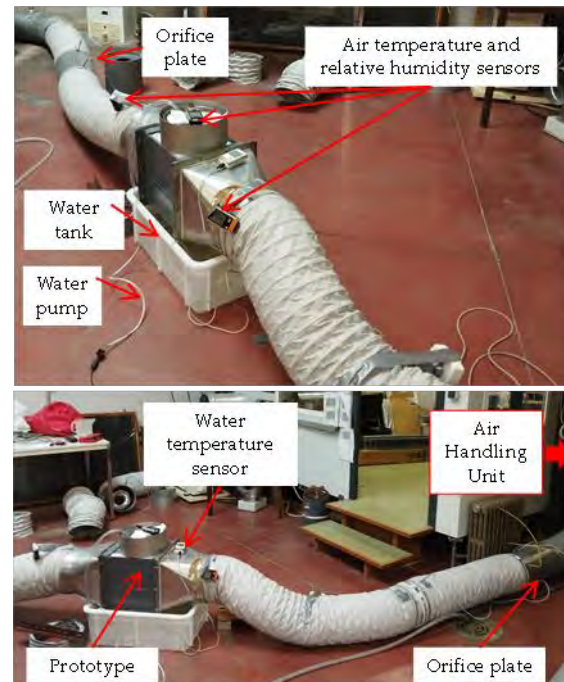


Fig. 5 – Test bench (the air handling unit is not visible)

The experiments are performed by connecting the prototype to an air handling unit that controls the inlet air conditions. Some sensors measure the temperature and relative humidity of the inlet primary air, the outlet primary air, and the outlet sec-

ondary air. Furthermore, the total air mass flow-rate and the primary air mass flow-rate were measured indirectly by measuring the pressure drop between two orifice plates located respectively before and after the prototype. However, the secondary air mass flow is calculated through the difference between total and primary air mass flow-rate. The operative range and the accuracy of the sensors are reported in Table 2.

The tests are repeated three times, by setting the inlet air temperature at 30 °C, 35 °C, and 40 °C. The measures are taken after 20 minutes to enhance the steady state conditions. The inlet humidity ratio is 13.2 ± 0.8 g/kg, the total air volume flow is 6.25 ± 0.27 m³/min, the working-to-intake air ratio is about 0.42.

Table 2 – Operative range and accuracy of sensors

Sensor	Range	Accuracy
Static pressure	0/25 hPa	± 0.02 hPa or $\pm 1\%$
Dry bulb temperature	-20/+55°C	± 0.4 °C
Air relative humidity	0/100%	$\pm 2\%$ RHat +25 °C

2.5 Calculation of the overall heat transfer coefficient

The overall heat transfer coefficient K between wet and dry channels is calculated as in Eq. 12:

$$K = \frac{1}{\frac{1}{\alpha_{dry}} + R_{wall} + \frac{1}{\alpha_{wet}}} \quad (12)$$

Here, R_{wall} is the thermal resistance of the channel wall and is considered negligible due to the small thickness of both the polycarbonate plate and the cloth. Instead, α_{dry} and α_{wet} are the convective heat transfer coefficients in the dry and the wet side, respectively, determined as reported in Eq. 13.

$$\alpha = \frac{Nu}{D_{eq}} \lambda \quad (13)$$

with λ thermal conductivity of the air, $D_{eq} = 4S/P$ the equivalent diameter (being S the transversal section of the channel and P the corresponding perimeter). The equivalent diameter is 9 mm for the dry channel and 19 mm for the wet channel.

The Nusselt Number (Nu) is calculated by considering different sources (Jie & Chua, 2023; Deepak et al., 2022; Kashyap et al., 2020).

According to (Jie & Chua, 2023), the Nusselt Number in a dry channel Nu_{dry} is calculated from the following equations:

$$Nu_{dry} = \frac{\frac{Nu_0}{\tanh(2.264Gz^{\frac{1}{3}} + 1.7Gz^{\frac{2}{3}})} + 0.0499Gz \tanh(Gz^{-1})}{\tanh(2.432Pr^{1/6}Gz^{-1/6})} \quad (14)$$

$$Nu_0 = \frac{48}{11} \quad (15)$$

$$Gz = \frac{D_{eq}}{L} Re Pr \quad (16)$$

Where Re and Pr are the Reynolds and Prandtl numbers respectively, while D_{eq} is the hydraulic diameter and L is the channel length.

The Nusselt Number inside the wet channel Nu_{wet} , however, must be calculated as follows:

$$Nu_{wet} = 0.10 \left(\frac{L_w}{\delta} \right)^{0.12} Re_{L_w}^{0.8} Pr^{1/3} \quad (17)$$

$$Re_{L_w} = \frac{\rho v}{\mu} L_w \quad (18)$$

Where L_w is the thickness of the water film– that is not known and difficult to measure, thus its value is supposed as 0.5 mm – δ is the total thickness including the water film and the channel wall, and ρ , v , and μ are respectively the density, velocity, and dynamic viscosity of the air in the wet channel.

However, (Jie & Chua, 2023) assumed a laminar flow regime, generalizing for all DPEICs because of the small section of the channels although a transition flow regime (Re between 2300 to 3500) is found out in the tested device for both wet and dry channels. Since the flow regime is very relevant in the description of the heat exchange (Gicquel, 2021), the model proposed by Jie and Chua might not be very accurate.

Even though the hypothesis of laminar flow is very common in the literature, (Deepak et al., 2022) found out a turbulent flow regime, thus calculating the Nusselt Number with the following equation:

$$Nu = \frac{(f/8)(Re-1000)Pr}{1 + 12.7 \left(\frac{f}{8} \right)^{\frac{1}{2}} \left(Pr^{\frac{2}{3}} - 1 \right)} \quad (19)$$

$$f = (0.790 \ln(Re) - 1.64)^{-2} \quad (20)$$

Nevertheless, the same equation is used in both dry and wet channels, which may also make this model unreliable.

Finally, a different approach is used by (Kashyap et al., 2020), who proposed to use the value of relative velocity of the air with respect to the water film to calculate the Reynolds number in wet channels. In this case the flow regime is laminar, and the Nusselt Number is calculated as follows:

$$Nu = 2 + 0.6 \cdot Re^{0.5} Pr^{0.33} \quad (21)$$

Since it is not possible to know *a priori* the mean temperature of the primary and secondary air flow, the convective heat transfer coefficient is estimated as a function of the temperature for all models. In particular, the Nusselt number is calculated for the temperature of 280, 290, 300, 310 K and a linear function is derived from these values. Even if the variation of the convective heat transfer coefficient which derives by varying the temperature is not very significant, the function is still implemented in the model, for the sake of accuracy. The convective heat transfer coefficient as a function of the mean temperature in primary channel $T_{m1} = (T_{out1} - T_{in1})/2$ and in secondary channel $T_{m2} = (T_{out2} - T_{in2})/2$ is reported in table.

Table 3 – Calculated convective heat transfer coefficient as a function of the mean temperature in the channel

Model	Dry channel	Wet channel
Jie & Chua	$0.0174 \cdot T_{m1} + 27.034$	$-0.0127 \cdot T_{m2} + 5.9535$
Deepak et al.	$-0.124 \cdot T_{m1} + 34.496$	$-0.0563 \cdot T_{m2} + 12.92$
Kashyap et al.	$-0.0112 \cdot T_{m1} + 93.806$	$-0.0039 \cdot T_{m2} + 39.549$

3. Results and Discussion

3.1 Model Validation

According to the results of this study, the proposed model to simulate the DPIEC is more consistent with the experimental data in terms of outlet temperature prediction if the Nusselt number is calculated according to (Kashyap et al., 2020).

As reported in Fig. 6, all models tend to overestimate the outlet primary air temperature and underestimate the outlet secondary air temperature. However, the outlet secondary air temperature predicted by the model looks not consistent with experimental data, independently on the Nusselt number calculation. Indeed, the energy balance in Eq. 1 is not closed even by considering the experimental results. This is probably due to inaccuracies in the measurement of the outlet air temperature: in fact, the temperature probe on the air stream is slightly detached from the outlet section (Fig. 5) to avoid any chance that the water spray might wet

the sensor. In this way, the measure of the air temperature may be influenced by the air temperature of the laboratory that is warmer than the working air. This hypothesis will be verified in future experiments that will regard a larger and more realistic DPIEC model.

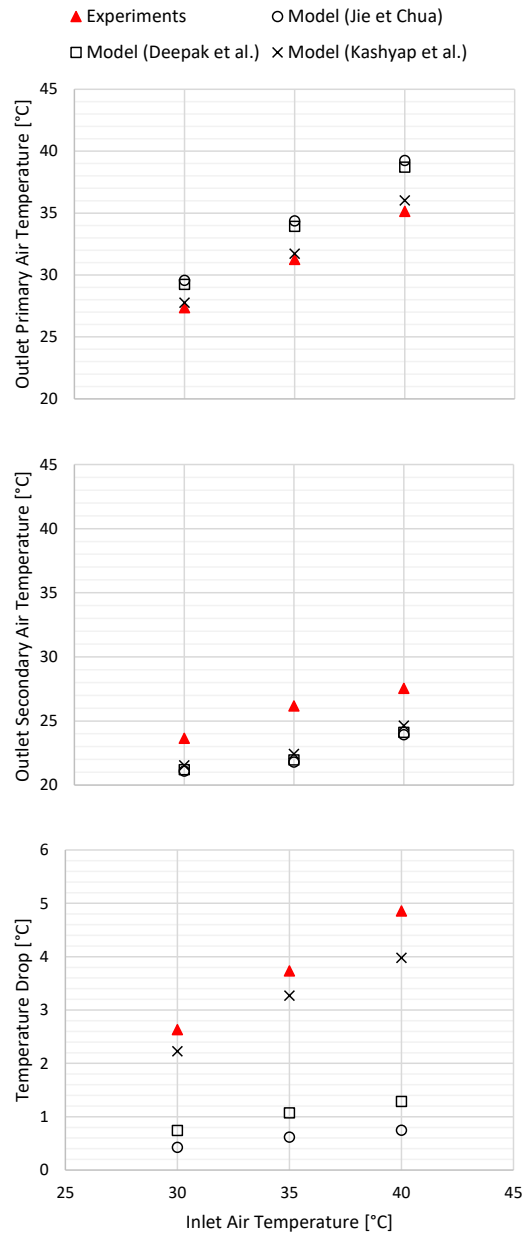


Fig. 6 – Model validation against experimental data. Outlet primary air temperature, outlet secondary air temperature, temperature drop

Looking at the temperature drop in the primary air – one of the most used parameters to evaluate the performance of DPIECs – the error in its prediction ranges between 12% and 18% with the model by

(Kashyap et al., 2020). In the other cases, the error is unacceptable: indeed, it reaches 85% if the Nusselt Number is calculated according to (Jie & Chua, 2023), while it reaches 74% by referring to (Deepak et al., 2022). In other terms, the accuracy of the proposed model –in terms of temperature drop – is significantly influenced by the method used to calculate the heat transfer coefficient between air and the channel surfaces. While the dry channel could be considered in the same way as a conventional heat exchanger channel, this is not true for the wet channels: here, the heat exchange between air and wall is more complex due to the presence of water. The method used by (Jie & Chua, 2023) tried to model the effect of water, but this could be inconsistent with the reality. For example, the determination of the thickness of the water film may be very difficult in practice. In fact, the water might not be uniformly spread in the wall of the wet channel. However, the inconsistency of the model is demonstrated by the experiments. Also, the hypothesis of laminar flow, although acceptable in several cases, could not be suitable for all DPIECs.

Furthermore, the wide discrepancy between different methods to determine the Nusselt Number reported in the literature on DPIEC reveals the importance of delving on this issue.

3.2 Parametric Analysis

The temperature drop ensured by the prototype ranges between 3 °C and 5 °C. This result may improve significantly by increasing the heat exchange surface. For this reason, based on the developed model, a parametric analysis is performed by changing the size of the device. The inlet conditions are set as follows: air temperature 35 °C, relative humidity 50%, air mass flow rate 0.1 kg/s, working-to-intake air ratio 0.42.

With respect to the original size, each of the main dimensions (length, height, and width) are duplicated and triplicated. The results are shown in Fig. 7 by considering the same inlet air conditions, the temperature drop can increase from 2.2 °C to 4.9 °C by increasing three times the dimensions of the device. While the effect of enlarging the height or the width does not produce a significative

difference, the augmentation of the length results in a minor temperature drop (4.2 °C against 4.9 °C).

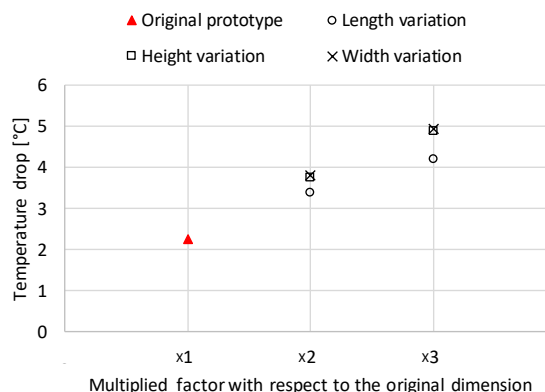


Fig. 7 – Effect of a variation of length, height, and width of the device

4. Conclusion

This paper aims to develop a mathematical model of a dew-point indirect evaporative cooler to easily implement it in TRNSYS building simulations. The model is based on the mass and energy balance equations and on the logarithmic mean temperature difference method. The model refers to a mixed-flow prototype; however, it can be applied to other DPIECs with different configurations and design characteristics, by determining the heat transfer area and the heat transfer coefficient of the heat and mass exchanger.

The model has been written in Python programming language, so that it can be called in TRNSYS Simulations Studio by Type 169. The implementation of the Python code in TRNSYS and the building performance analysis will be evaluated in future studies. In this paper, the mathematical model is validated against experimental data: the results show that the model is sufficiently consistent with the experiments with an error in the primary air temperature drop between 12% and 18%. The relatively important discrepancy is most probably due to the inaccurate position of the temperature probe on the outlet air stream and is also influenced by the small size of the prototype.

However, the current study reveals the importance of a proper calculation for the Nusselt Number, especially in the wet channel where heat exchange is more complex than in conventional heat exchang-

ers due to the presence of water: this suggests the need to better investigate the determination of the heat transfer coefficient in wet channels of DPIECs. In conclusion, a parametric study is performed to evaluate the effect of a variation of the length, the height, and the width of the device. With the same inlet air conditions, the temperature drop can increase from 2.2 °C to 4.9 °C by increasing three times the height or the width of the device. The increase in the length may be slightly less advantageous. However, the influence of the size should be evaluated carefully with respect to the technical possibility to ensure a uniform air distribution inside the channels, along with the necessity to create devices as compact as possible to save raw materials and make the installation easier.

Acknowledgement

This work has been developed within the research project TED2021-129652A-C22, funded by MCIN/AEI/10.13039/501100011033 and the European Union through the “NextGenerationEU”/PRTR.

Nomenclature

Symbols

A	Heat transfer area (m ²)
c	Specific heat (J/kgK)
D_{eq}	Equivalent diameter (m)
DPIEC	Dew Point Indirect Evaporative Cooler
f	Friction factor (-)
h	Enthalpy (J/kg)
K	Heat transfer coefficient (W/m ² K)
L	Channel length (m)
Lw	Thickness of the water film (m)
\dot{m}	Air mass flow-rate (kg/s)
Nu	Nusselt number (-)
Pr	Prandtl number (-)
R	Thermal resistance (m ² K/W)
Re	Reynolds number (-)
T	Temperature (°C)
x	Humidity ratio (kg/kg)
v	Air velocity (m/s)
α	Convective heat transfer coefficient (W/m ² K)

δ	Channel thickness (m)
ΔT_{lm}	Log mean temperature difference (°C)
η	Working to intake air ratio (-)
λ	Air thermal conductivity (W/mK)
μ	Air dynamic viscosity (kg/ms)
ρ	Air density (kg/m ³)

Subscripts/Superscripts

a	air
in	inlet
m	mean
out	outlet
v	vapor
w	water
1	primary
2	secondary

References

- Deepak, C., R. Naik, S. C. Godi, C. K. Mangrulkar and H. K. Prashanth. 2022. “Thermal performance analysis of a mixed-flow indirect evaporative cooler” *Applied Thermal Engineering* 217. doi:10.1016/j.applthermaleng.2022.119155
- Gicquel, Renaud. 2021. *Energy Systems: a new approach to Engineering Thermodynamics*. CRC Press
- Jie, Lin and Kian Jon Chua. 2023. *Indirect Dew-Point Evaporative Cooling: Principles and Applications*. Springer Charm. doi:10.1007/978-3-031-30758-4
- Kashyap, S., J. Sarkar, and A. Kumar. 2020. “Comparative performance analysis of different regenerative evaporative cooling device topologies” *Applied Thermal Engineering* 176. doi:10.1016/j.applthermaleng.2020.115474
- TRNSYS 18. *A TRaNsient System Simulation program. Mathematical references*. Volume 4